A Hybrid Model for Situation Monitoring and Conflict Prediction in Human Supervised “Autonomous” Systems

Charles Lesire and **Catherine Tessier**
ENSAE-Supaero, Toulouse, France
Onera-DCSD, Toulouse , France
{lesire,tessier}@onera.fr

Abstract

The paper focuses on a key issue for human supervised “autonomous” systems, namely situation monitoring. The operator’s involvement within human-robot team is first described as the way they close the control and decision loops. Then a framework based on particle filtering and Petri nets is presented for hybrid numerical-symbolic situation monitoring and inconsistency and conflict prediction within the team.

Human-robot team and the operator’s involvement

Autonomy is not an end in itself in robotic systems. Autonomy is needed because we want robots to be able to cope with mission hazards when communications with the human operator are impossible (due to communication gaps, discretion requirements, or to the operator’s workload). Therefore adjustable autonomy must be considered to enable the robots to compensate for the operator’s *neglect* (Goodrich *et al.* 2001). The control of shared autonomy may be human-initiated, *a priori* scripted or robot-initiated (Brookshire, Singh, & Simmons 2004). Whatever the case, implementing adjustable autonomy requires situation awareness (Endsley 2000) – including predicting what is likely to happen next – both from the operator’s and robot’s points of view (Drury, Scholtz, & Yanco 2003).

A functional architecture that is worth considering when dealing with autonomy and operator’s roles within a human-robot team is the *double loop* (Barrouil 1993), which parallels the symbolic decision loop (situation monitoring and replanning) with the classical numerical loop (estimation and control) - see Fig. 1.

Many papers have suggested autonomy levels for robots (Huang *et al.* 2004), human-agent teamwork (Bradshaw *et al.* 2003), UAVs[1] (Clough 2002) and others have focused on the operator’s roles (Yanco & Drury 2002; Scholtz 2003). What we are suggesting here is that the operator’s involvement can be regarded as the way they “close” the loops (Fong, Thorpe, & Baur 2003). Let us distinguish three main autonomy levels for a single robot or UAV agent:

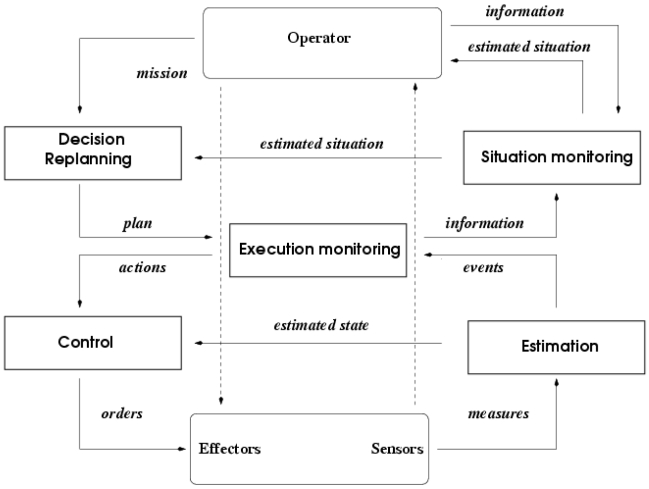

Figure 1: Functional architecture of autonomous systems - the double loop (Decisional autonomy (b))

1. **No autonomy**
   the operator closes the numerical loop *via* direct perception from sensors and direct action on effectors (teleoperation);
2. **Operating autonomy**
   (a) the operator closes the numerical loop *via* control laws (e.g. heading, slope, speed, altitude...)
   (b) waypoints are defined; the operator monitors the execution (checks whether the waypoints are correctly reached) and deals with failures, i.e. embodies the whole decision loop;
3. **Decisional autonomy**
   (a) waypoints are recalculated autonomously if forbidden areas appear in the course of the mission; the operator is highly involved within the decision loop, i.e. inputs area features, checks whether recalculated waypoints are OK and deals with other failures;
   (b) autonomous situation assessment and replanning are performed; the operator may close the decision loop when needed and when possible (i.e. when communications are available).

[1] Uninhabited Aerial Vehicles.

Remark 1 *The operator closes the numerical or decision loop provided required communications with the robot are available.*

Remark 2 *In case of emergency, a manual handover may be possible (provided required communications are available).*

Situation monitoring is a key issue in human-robot teams: indeed situation monitoring has to maintain both the operator's situation awareness and situation assessment for the robot (Drury, Scholtz, & Yanco 2003), so that the task context should not be lost when the robot cedes control to the human or conversely (Brookshire, Singh, & Simmons 2004). What is more is that the global human-robot team must be predictible whatever may occur, e.g. failures, operator's omissions or wrong moves. Therefore what is needed is a global situation monitoring to track and predict the behaviour of the human-robot team, according to the human's involvement into the control loops, and possibly detect inconsistencies within the team.

As it is already clear with the double-loop representation (see Fig. 1), human-robot team are hybrid systems, in so far as both numerical (continuous) and symbolic (discrete) parts are involved. It must be noticed that the discrete part is not a mere abstraction of the continuous part - as it is the case in most of the hybrid system literature: indeed the discrete part mostly corresponds to how the operator interacts with the robot and sets configurations or modes.
What is presented in the paper is a way to estimate and predict the states in such hybrid systems through a unified model, and how conflicts (possibly leading to dangerous situations) may be predicted within the team.

After an overview of hybrid system estimation methods, the particle Petri net - a joint model for situation monitoring in hybrid systems - will be presented. Afterwards the estimation principles will be described and illustrated on the thermostat example. Finally the application of particle Petri net-based estimation to situation monitoring in human supervised "autonomous" systems will be dealt with.

Hybrid State Estimation

Estimating the state of a hybrid system is widely studied in the literature and involves a large amount of techniques, from numerical filters to network models.

In (Veeraraghavan & Papanikolopoulos 2004) the estimation rests on a set of Kalman filters, each one tracking a linear mode of the system. The most probable states allow to determine the most probable filter and then the most probable mode of the system (i.e. the most probable behavior of a car like turning, accelerating, etc.) In the same way, (Koutsoukos, Kurien, & Zhao 2003) propose an estimator based both on hybrid automata to represent the mode evolution and on a particle filter to estimate the continuous state of the system. The estimated mode is then the most probable mode of the system with respect to the estimated continuous states. A similar principle is applied in (Hofbaur & Williams 2002) who use a concurrent probabilistic hybrid automaton (cPHA) to estimate the mode of the system using Kalman filters.

Bayesian networks are also used to represent hybrid systems by modeling the links between discrete and continuous variables in terms of conditional probabilities over time. Inference rules (Lerner & Parr 2001) or particle filtering (Doucet *et al.* 2000) can be used to estimate the state of a hybrid system. However Bayesian networks suffer from:

1. the necessity to define a measure (probability, possibility…) on the (continuous and discrete) state. This is sometimes impossible to do for instance in case of complete uncertainty (see (Chachoua & Pacholczyk 2000));
2. the fact that an analysis on the consistency of the discrete and continuous states is difficult to perform as the estimations on discrete and continuous states are aggregated within the probability distribution.

In the same way, the analysis of conflicts, or conversely consistency, is mainly based on the study of continuous variables. In (Benazera & Travé-Massuyès 2003) the hybrid system must satisfy constraints that are checked on the continuous estimated states of the system. (Del Vecchio & Murray 2004) use lattices to identify the discrete mode of a hybrid system when only continuous variables are observed. In (Tomlin *et al.* 2003), the reachability analysis of continuous states, based on hybrid automata, allows to identify safe and dangerous behaviors of the system and is applied to an aircraft collision problem. Nielsen and Jensen (Nielsen & Jensen 2005) define a conflict measure on the estimated state of a Bayesian network; nevertheless this method still suffers from the need to define a measure on totally uncertain states, and from the fact that the conflict measure is continuous, which leads to a threshold effect. In (Lesire & Tessier 2005) an aircraft procedure and pilot's actions are jointly modeled using a *particle Petri net* that allows the procedure to be simulated using a Monte-Carlo method and the results to be analysed using the Petri net properties. Hence only the nominal procedure is modeled and the analysis is based on qualitative properties and does not involve any continuous measure.

The monitoring system presented in this paper is based on the later work: it allows both the estimation to be computed and the consistency of the estimated states to be analysed without defining *a priori* measures on unknown states. Indeed it is the structure of the Petri net-based model itself which allows the consistency to be checked. The next section mentions the main definitions of particle Petri nets.

Particle Petri Nets

Prerequisites

Particle Filtering The particle filter (Arulampalam *et al.* 2002) allows the state x_k at time k of a dynamic system subject to deterministic and random inputs to be estimated from observations z_k spoilt with stochastic errors. It is based on a discretization of the uncertainty on the state value: the probability distribution function of the estimate $\hat{x}_{k|k}$ – meaning the state estimated at time k knowing the observation at time

k – is represented by a set of N particles $x^{(1)}_{k|k}, \ldots, x^{(N)}_{k|k}$ (see Fig. 2). The estimation is achieved through a two-step process : the *prediction*, that consists of estimating the next particles $x^{(i)}_{k+1|k}$ according to the evolution model, and the *correction*, that is based on a comparison of the expected particle values with the observation: the closer the expected particles are to the most probable value of the observation, the bigger weight they are assigned. Then N new particles $x^{(i)}_{k+1|k+1}$ are generated from a resampling of the weighted corrected particles.

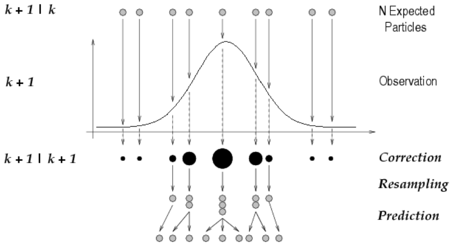

Figure 2: Particle filtering (from (Lehmann 2003))

Petri Nets A Petri net $< P, T, F, B >$ is a bipartite graph with two types of nodes: P is a finite set of places; T is a finite set of transitions (David & Alla 2005). Arcs are directed and represent the forward incidence function $F : P \times T \rightarrow \mathbb{N}$ and the backward incidence function $B : P \times T \rightarrow \mathbb{N}$ respectively. An *interpreted Petri net* is such that conditions and events are associated with places and transitions. When the conditions corresponding to some places are satisfied, tokens are assigned to those places and the net is said to be marked. The evolution of tokens within the net follows transition firing rules. Petri nets allow sequencing, parallelism and synchronization to be easily represented.

Particle Petri Nets

A *particle Petri net* (Lesire & Tessier 2005) is a hybrid Petri net model where places and transitions are either numerical or symbolic:

1. *numerical places* P_N are associated with differential equations representing the continuous evolution of the system;
2. *numerical transitions* T_N are associated with conditions and represent mode changes in the system dynamics;
3. *symbolic places* P_S and *transitions* T_S are associated with symbolic states and actions respectively.

The state of the system is represented by a set of tokens, that are *particles* $\pi^{(i)}_{k+1|k}$ – meaning particle number i at time $k + 1$ knowing the observation at time k –, evolving within the numerical places, and a set of *configurations* $\delta^{(j)}_{k+1|k}$ evolving within symbolic places. A marking $m_{i,j} = (\pi^{(i)}, \delta^{(j)})$ represents a possible state of the system. The firing rules (Lesire & Tessier 2005) associated with numerical and symbolic transitions allow all the expected states of the system to be computed whatever the actions.

Figure 3 is the particle Petri net of a thermostat. The thermostat manages temperature[2] θ between $20°C$ and $25°C$. The numerical places p_0, p_1 and p_2 are associated with differential equations modeling heating ($\dot{\theta} = -0.2\theta + 5.4$) and cooling ($\dot{\theta} = -0.1\theta + 1.2$) respectively. The numerical transitions correspond to guards: transitions $\theta > 25$ and $\theta < 20$ indicate respectively that the temperature is and is not warm enough. The symbolic places indicate the modes of the thermostat (*on* or *off*) and the symbolic transitions (OFF) represent external actions to turn off the thermostat.

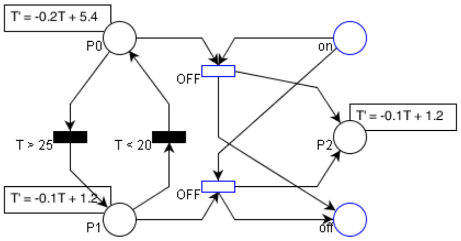

Figure 3: The thermostat particle Petri net

Estimation principles

The estimator presented here is based on the particle filtering principle and computes the expected markings of a particle Petri net. The estimation is achieved through a two-step process:

1. a prediction of the expected markings, according to the particle Petri net firing rules, that computes all the possible combinations of numerical and symbolic states;
2. a correction of the markings according to an observation made on the system.

Prediction

The prediction is achieved through the computation of the *reachable markings* of the particle Petri net, i.e. the set of the expected states. It is based both on an *isoparticle evolution*, i.e. an evolution of the tokens within the net to model mode changes according to actions, and an *isomarking evolution*, i.e. an evolution of the particles according to differential equations.

Let us consider the example of the thermostat (Fig. 3), and let the initial marking be $\pi^{(0)}_{0|0} = 20°C$ marking place p_0 and $\delta^{(0)}$ marking place on. Then the expected marking at time 1 is the marking shown on Fig. 4, where

1. in place p_0, particle $\pi^{(0)} = 21.4°C$ has evolved according to the heating differential equation;

[2] The temperature is noted θ in the text and T on figures as the θ character is not available in the estimation software and T is already the set of transitions of the particle Petri net.

2. in place p_2, particle $\pi^{(1)} = 19.2°C$ has evolved according to the cooling differential equation, predicting the situation corresponding to the thermostat being turned off;
3. configurations $\delta^{(0)}$ and $\delta^{(1)}$ in symbolic places *on* and *off* respectively indicate that the thermostat may be either on or off at time 1.

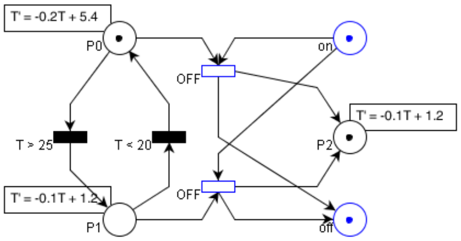

Figure 4: Predicted marking at time 1

Thereby the marking at time k represents the estimated states as a set of tokens – the set of particles being a discretization of the probability distribution on the continuous state –, and the prediction step computes the expected marking at time $k+1$.

Correction

The correction consists in comparing matchings between the predicted tokens and the incoming observation and selecting the "best" ones. The correction process:

1. weights the predicted particles according to the noisy observation:

$$w(\pi^{(i)}_{k+1|k}) = \frac{p(z_{k+1}|\pi^{(i)}_{k+1|k})}{\sum_{j=0}^{N} p(z_{k+1}|\pi^{(j)}_{k+1|k})} \tag{1}$$

   where z_{k+1} is the observation at time $k+1$, $w(\pi)$ is the weight of particle π and $p(z|\pi)$ is the conditional probability to observe z knowing the expected state π;

2. groups the weighted particles according to the equivalence relation $\mathcal{R}$:

$$\pi^{(i)}\mathcal{R}\pi^{(j)} \Leftrightarrow \begin{cases} \forall p \in P_N, (\pi^{(i)} \in \mathcal{M}(p) \Leftrightarrow \pi^{(j)} \in \mathcal{M}(p)) \\ \forall \pi^{(k)} \in \Pi \;/\; \forall p \in P_N (\pi^{(i)} \in \mathcal{M}(p) \Rightarrow \pi^{(k)} \notin \mathcal{M}(p)), \\ \qquad (w(\pi^{(i)}) \geq w(\pi^{(k)}) \Leftrightarrow w(\pi^{(j)}) \geq w(\pi^{(k)})) \end{cases} \tag{2}$$

   where $\Pi = \{\pi^{(i)}, i \in [\![1;N]\!]\}$ and $\mathcal{M}(p)$ is the marking of place p. The equivalence classes are noted $\Gamma = \{\gamma^{(i)}_{k+1|k}\}$, and their weights are defined by

$$w(\gamma^{(i)}_{k+1|k}) = \sum_{\pi \in \gamma^{(i)}_{k+1|k}} w(\pi) \tag{3}$$

   The process is then recursively applied on Γ to group the equivalence classes until they are restricted to singletons;

   Remark 3 *The equivalence relation $\mathcal{R}$ is designed to help diagnose the state of the system by reducing the size of the data to be analysed. (2) means that particles $\pi^{(i)}$ and $\pi^{(j)}$ are equivalent if they mark the same place p and for each particle $\pi^{(k)}$ which is not in p, both $\pi^{(i)}$ and $\pi^{(j)}$ have either a higher or lower weight than $\pi^{(k)}$.*

   Remark 4 *The algorithm applying recursively relation $\mathcal{R}$ on particles and then on equivalence classes terminates and computes at most N steps, where N is the number of particles (the worst case considers that at each step only two classes are equivalent).*

3. updates (Benferhat, Lagrue, & Papini 2005) the ranking of predicted configurations $\delta_{k+1|k}$ according to the observation. This results in a ranking of corrected configurations $\delta_{k+1|k+1}$ ($\prec_\Delta$ means "is preferred to"):

$$(z_{k+1} \rightarrow \delta^{(i)}_{k+1|k}) \wedge (z_{k+1} \not\rightarrow \delta^{(j)}_{k+1|k}) \Rightarrow \delta^{(i)}_{k+1|k+1} \prec_\Delta \delta^{(j)}_{k+1|k+1} \tag{4}$$

   where $z \rightarrow \delta$ means that configuration δ matches observation z (see Example 1 below). (4) means that the configurations matching the observation are preferred to the configurations not matching the observation.

   If both $\delta^{(i)}_{k+1|k}$ and $\delta^{(j)}_{k+1|k}$ match (or do not match) the observation, the ranking is not changed, the relation between $\delta^{(i)}_{k+1|k+1}$ and $\delta^{(j)}_{k+1|k+1}$ is the same as between $\delta^{(i)}_{k+1|k}$ and $\delta^{(j)}_{k+1|k}$:

$$\begin{aligned} &(z_{k+1} \rightarrow \delta^{(i)}_{k+1|k} \wedge z_{k+1} \rightarrow \delta^{(j)}_{k+1|k}) \\ &\qquad \Rightarrow (\delta^{(i)}_{k+1|k+1} \precsim_\Delta \delta^{(j)}_{k+1|k+1} \Leftrightarrow \delta^{(i)}_{k+1|k} \precsim_\Delta \delta^{(j)}_{k+1|k}) \end{aligned} \tag{5}$$

$$\begin{aligned} &(z_{k+1} \not\rightarrow \delta^{(i)}_{k+1|k} \wedge z_{k+1} \not\rightarrow \delta^{(j)}_{k+1|k}) \\ &\qquad \Rightarrow (\delta^{(i)}_{k+1|k+1} \precsim_\Delta \delta^{(j)}_{k+1|k+1} \Leftrightarrow \delta^{(i)}_{k+1|k} \precsim_\Delta \delta^{(j)}_{k+1|k}) \end{aligned} \tag{6}$$

   The relation $\precsim_\Delta$ (meaning "is preferred or equivalent to") is a partial preorder on the set of configurations;

   Example 1 *In the thermostat example, relation $\rightarrow$, representing the matching between predicted configurations and the observation, is defined by :*

   (a) on $\rightarrow$ on *and* on $\not\rightarrow$ off,

   (b) off $\rightarrow$ off *and* off $\not\rightarrow$ on,

   (c) on $\wedge$ off $\rightarrow$ on *and* on $\wedge$ off $\rightarrow$ off

   (d) false $\rightarrow$ on *and* false $\rightarrow$ off

   where case (c) corresponds to an observation of both modes on *and* off*, that may come from a sensor error, and case (d) corresponds to an empty observation (*false*) that may come from a sensor failure.*

4. constructs the *correction graph* by ranking (relation $\precsim$) the markings $m_{i,j} = (\gamma^{(i)}, \delta^{(j)})$, according to the weights on $\gamma^{(i)}$ and to relation $\precsim_\Delta$ on configurations $\delta^{(j)}$:

$$m_{i,j} \prec m_{k,l} \quad \Leftrightarrow \quad \begin{cases} w(\gamma^{(i)}) \geq w(\gamma^{(k)}) \wedge \delta^{(j)} \precsim_\Delta \delta^{(l)} \\ w(\gamma^{(i)}) > w(\gamma^{(k)}) \vee \delta^{(j)} \prec_\Delta \delta^{(l)} \end{cases} \tag{7}$$

$$m_{i,j} \sim m_{k,l} \quad \Leftrightarrow \quad (\, w(\gamma^{(i)}) = w(\gamma^{(k)}) \wedge \delta^{(j)} \sim_\Delta \delta^{(l)} \,) \tag{8}$$

5. resamples the particles : N new particles $\pi^{(i)}_{k+1|k+1}$ are drawn from the discrete probability law $\{\pi^{(i)}_{k+1|k}, w(\pi^{(i)}_{k+1|k})\}$. The particles are then spoilt with the model noise to represent the model approximation.

The resampled particles represent the estimated numerical states of the system at time $k+1$ and are introduced in the next prediction step. The correction graph built from predicted tokens is analysed to detect inconsistencies. This analysis is presented in the next section. The whole estimation process is illustrated through the thermostat example.

Consistency Analysis and Conflict Detection

A state of the system is said to be consistent if it is a possible state with respect to the initial state and to the model of the nominal behavior of the system. The set of possible states can be computed before the on-line estimation and consists in computing the reachable states of the particle Petri net.

Hence an ordinary safe Petri net[4] is associated with the particle Petri net of the system such as one ordinary token is associated to each place corresponding to a marked (by particles or by configurations) place in the particle Petri net.

Let the initial marking of the ordinary safe Petri net of the thermostat (Fig. 3) be $\mathcal{M}_0 = (1\,0\,0\,1\,0)$: places p_0 and *on* are marked, places p_1, p_2 and *off* are empty. Then marking $\mathcal{M}_0$ represents the initial state of the Petri net: the thermostat is on and heating.

The reachable states of the particle Petri net correspond to the *reachable markings* of the safe Petri net represented in Fig. 5. The graph of reachable markings is the classical automaton of a thermostat, with three modes: *on* (marking $\mathcal{M}_0$), *idle* (marking $\mathcal{M}_1$) and *off* (marking $\mathcal{M}_2$). Consequently the markings that are inconsistent in the estimation process are:

1. $\mathcal{M}_4 = (0\,0\,1\,1\,0)$, meaning that the thermostat is *on* but the temperature decreases;
2. $\mathcal{M}_5 = (1\,0\,0\,0\,1)$, meaning that the thermostat is *off* but is still heating;
3. $\mathcal{M}_6 = (0\,1\,0\,0\,1)$, meaning that the thermostat is *off* but will heat as soon as the temperature is under 20.

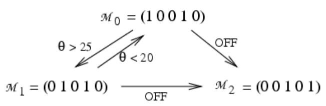
$\mathcal{M}_0$ = (1 0 0 1 0)
θ > 25
θ < 20
OFF
$\mathcal{M}_1$ = (0 1 0 1 0)
OFF
$\mathcal{M}_2$ = (0 0 1 0 1)

Figure 5: Reachable markings of the thermostat Petri net

Remark 5 *The computation of the reachable markings may be complex in general as the set of reachable markings may be infinite. Nevertheless the set of reachable markings of a safe Petri net is finite.*

The consistency analysis is achieved through the study of the correction graph computed during the correction process:

1. Each marking $m_{i,j} = (\gamma^{(i)}, \delta^{(j)})$ is associated with a marking $\widetilde{m}_{i,j}$ in the associated safe Petri net:

$$\forall p\in P=P_N\cup P_S,\quad \widetilde{m}_{i,j}(p)=\begin{cases}1 \text{ if } \gamma^{(i)}\in\mathcal{M}(p)\text{[5]} \text{ or } \delta^{(j)}\in\mathcal{M}(p)\\ 0 \text{ otherwise}\end{cases} \tag{9}$$

2. Then the consistency of $m_{i,j}$ is checked:

$$m_{i,j} \text{ is consistent } \Leftrightarrow \widetilde{m}_{i,j} \in \mathcal{G} \tag{10}$$

where $\mathcal{G}$ is the graph of the reachable markings of the safe Petri net.

Knowing the (in)consistent markings of the correction graph is a first step towards the detection of conflictual situations. Some issues in analysing such a graph are currently under study, for instance about using the graph in the resampling strategy or identifying patterns in the correction graph to detect well-known conflictual situations.

The next section presents some examples and results about the estimation principle and the consistency analysis.

Simulations

Thermostat Monitoring

The initial marking of the thermostat is represented in Fig. 6 where 50 particles have been drawn from the normal distribution $\mathcal{N}(22°C, 1)$ – $22°C$ is the initially observed temperature.

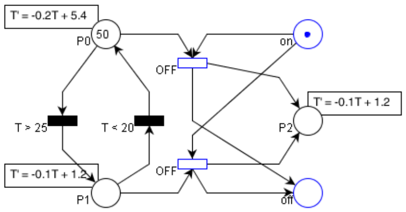

Figure 6: Initial estimated state of the thermostat: the thermostat is on, heating, and the temperature is approximatively $22°C$.

Temperature Estimation Figure 7 is the result of the estimation process launched on the Petri net of Fig. 6 with a new observation of the temperature and the thermostat mode every second. The dashed line represents the (noisy) observations and the crosses are the particles.

We can notice that the shape of the estimated temperature smoothly fits the observed temperature, meaning that the estimation well corresponds to the thermostat behavior. To illustrate the estimation process, let us consider the correction step at time 1.

[4] An ordinary Petri net is a Petri net with no interpretation containing undifferentiated classical tokens. A Petri net is said to be *safe* for an initial marking $\mathcal{M}_0$ if for all reachable markings, each place contains zero or one token.

[5] By abuse of notation, $\gamma^{(i)} \in \mathcal{M}(p)$ means that all the particles in $\gamma^{(i)}$ are marking place p (which is true by construction of $\gamma^{(i)}$).

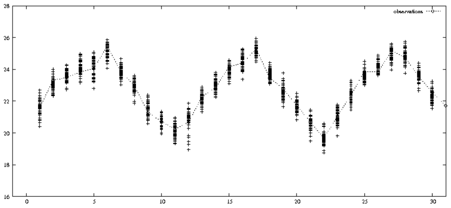

Figure 7: Estimation of the temperature

particle number	θ	weight	place
11	21.581	0.0361	p_2
12	21.594	0.0360	p_0
25	21.535	0.0360	p_0
41	21.615	0.0357	p_2
17	21.618	0.0357	p_0
18	21.624	0.0355	p_2
8	21.630	0.0354	p_0
29	21.502	0.0353	p_0
1	21.638	0.0352	p_0
42	21.642	0.0351	p_0

Table 1: Best weighted particles at time 1

The observation at time 1 is $z_1 = (21.567°C, on)$. Table 1 contains the ten best predicted particles according to z_1 and their associated weights. As far as the consistency analysis is concerned, it is easily guessed that analysing the whole table, containing fifty columns (one per particle), is not obvious. Then the particles are grouped in equivalence classes according to relation $\mathcal{R}$ applied recursively: when the particles are ranked by weight, (2) consists in making classes by grouping the particles by place following the ranking. The first step of the construction results in the following equivalence classes:

1. $\gamma^{(1)} = \{\pi^{(11)}\}$ with weight 0.0361 in p_2,
2. $\gamma^{(2)} = \{\pi^{(12)}, \pi^{(25)}, \pi^{(17)}\}$ with weight 0.1077 in p_0,
3. $\gamma^{(3)} = \{\pi^{(41)}, \pi^{(18)}\}$ with weight 0.0702 in p_2,
4. $\gamma^{(4)} = \{\pi^{(8)}, \pi^{(29)}, \pi^{(1)}, \pi^{(42)}\}$ with weight 0.1410 in p_0.

Relation (2) applied recursively on $\Gamma = \{\gamma^{(1)}, \gamma^{(2)}, \gamma^{(3)}, \gamma^{(4)}\}$ gives as a final result:

1. $\gamma^{(5)} = \{\gamma^{(4)}, \gamma^{(2)}\}$ with weight 0.2487 in p_0,
2. $\gamma^{(6)} = \{\gamma^{(3)}, \gamma^{(1)}\}$ with weight 0.1063 in p_2.

The associated correction graph is drawn in Fig. 8 where $\delta^{(0)} = on$ and $\delta^{(1)} = off$: as the observation is *on*, $\delta^{(0)} \prec \delta^{(1)}$, and as $w(\gamma^{(5)}) > w(\gamma^{(6)})$, the marking relation is $m_{5,0} \prec m_{5,1}$, $m_{5,0} \prec m_{6,0}$, $m_{5,0} \prec m_{6,1}$, $m_{5,1} \prec m_{6,1}$ and $m_{6,0} \prec m_{6,1}$.

The framed markings are consistent. As a result, the best marking (the root of the graph) is consistent and matches the *on* state (thermostat on and heating).

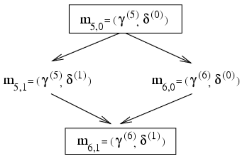
$m_{5,0} = (\gamma^{(5)}, \delta^{(0)})$
$m_{5,1} = (\gamma^{(5)}, \delta^{(1)})$
$m_{6,0} = (\gamma^{(6)}, \delta^{(0)})$
$m_{6,1} = (\gamma^{(6)}, \delta^{(1)})$

Figure 8: Correction graph at time 1

Inconsistent Behaviors In order to study the consistency of the thermostat behavior, two faulty cases are considered. Both consist in a wrong behavior of the thermostat that stops heating at temperatures $26°C$ and $24°C$ respectively.

Case 1: Figure 9 is the result of the estimation of the thermostat that stops heating at $26°C$. At time 7, the best marking (given the observation at time 7) has a weight of 0.9985 and matches the state *idle* (places p_1 and *on*). At time 8, the best marking has a weight of 0.9970 and matches the state *on* (places p_0 and *on*). The difficulty to estimate the right state can be explained by the fact that the behavior is misunderstood by the estimator as no particle has a temperature around $26°C$. At time 22, the best marking matches the *idle* state (place p_1 and *on*) with a weight of 1. Then from time 23, the best markings match state *off* (places p_2 and *off*) and consequently are inconsistent as the observation is *on*. The difficulty to track the behavior results in the fact that the estimation is completely wrong: all the particles are out of the main part of the Gaussian observation – 99% of the probability of a Gaussian distribution is within $[\mu - 3\sigma; \mu + 3\sigma]$ where μ is the mean value and σ the standard deviation.
This case shows that the prediction does not match the observations very well as nearly no particle has a temperature around $26°C$. Nevertheless the estimation is able to track the temperature over $25°C$. Switching from consistent to inconsistent matchings (times 7 and 8) reveals an inconsistent behavior.

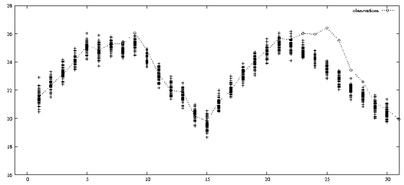

Figure 9: Conflict detection: the behavior of the thermostat is unknown.

Case 2: Figure 10(a) is the result of the estimation of the thermostat that stops heating at $24°C$. In that case the estimation is completely different: all the correction graphs from time 4 are the same (Fig. 10(b), where $\gamma^{(1)} \in p_2$). Indeed the numerical observations can be explained as they match the particles within place p_2. However the symbolic observation is *on*. Then the best corrected marking is inconsistent and reveals a fault: the temperature evolves as if the thermostat was off.

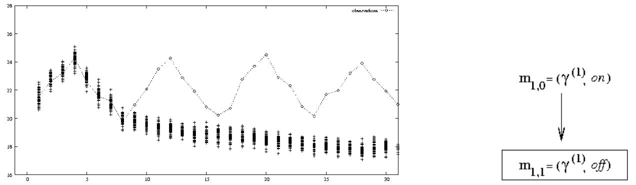

(a) Estimation of the temperature

(b) Correction graph

Figure 10: Conflict detection: the behavior of the thermostat corresponds to the *off* mode.

Estimation of the UAV-Operator Activities

This section presents an application of the estimation principle to a human–UAV team. This could be easily generalized to any human–robot or human–system team involving procedures (e.g. the Water Recovery System (Martin, Schreckenghost, & Bonasso 2004)). The considered mission is modeled by the particle Petri net of Fig. 11 and consists of an Approach from waypoint A to waypoint B where actions are shared between the UAV and the operator.

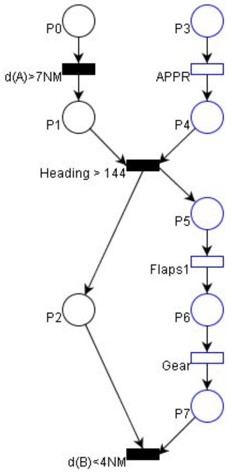

Figure 11: The particle Petri net of the Survey mission

Numerical places and transitions represent the trajectory of the UAV. The procedure consists of a descent (place p_0) from waypoint A. At 7 NM from A (transition *d(A)>7NM*), the UAV starts turning (place p_1) and when intercepting heading 144° (transition *Heading>144*), the UAV has to perform a deceleration (place p_2). At 4 NM from B (transition *d(B)<4NM*), the Approach procedure is finished: the next phase is the Landing procedure. The symbolic transitions correspond to operator or UAV actions: pressing the APPR button (transition APPR while descending or turning) is an operator's action, setting flaps 1 and setting the gear down (transitions Flaps1 and Gear while decelerating) are autonomous actions of the UAV. Then the configurations have attributes *APPR*, *Flaps1* and *Gear*. The particles have attributes x, y, z (the 3-D coordinates of the UAV), s (the speed) and h (the heading).

The estimation of the UAV position (x and y coordinates) is represented in Fig. 12. The dashed lines represent the nominal trajectory of the UAV and the dots represent the estimated particles.

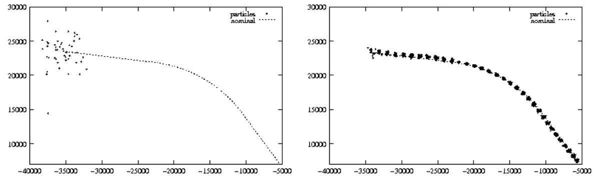

(a) at time 0

(b) from time 10

Figure 12: Estimation of the UAV position

At time 0, the UAV position is quite uncertain: the initial distribution is diffuse. The estimation becomes more precise from time 10.

At time 220, some particles mark place p_2 (the UAV may be decelerating) but the main corrected state matches place p_1: the UAV is still turning. At this time the observation states that the APPR button is not pressed. The correction graph at time 220 is shown in Fig. 13, with $\gamma^{(i)} \in p_i$ for $i \in \{1, 2\}$ and $\delta^{(j)} \in p_j$ for $j \in \{3, 4, 5, 6, 7\}$.

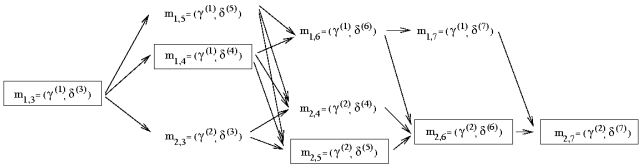
$m_{1,3} = (\gamma^{(1)}, \delta^{(3)})$
$m_{1,5} = (\gamma^{(1)}, \delta^{(5)})$
$m_{1,4} = (\gamma^{(1)}, \delta^{(4)})$
$m_{2,3} = (\gamma^{(2)}, \delta^{(3)})$
$m_{1,6} = (\gamma^{(1)}, \delta^{(6)})$
$m_{2,4} = (\gamma^{(2)}, \delta^{(4)})$
$m_{2,5} = (\gamma^{(2)}, \delta^{(5)})$
$m_{1,7} = (\gamma^{(1)}, \delta^{(7)})$
$m_{2,6} = (\gamma^{(2)}, \delta^{(6)})$
$m_{2,7} = (\gamma^{(2)}, \delta^{(7)})$

Figure 13: Correction graph of the mission at time 220

Marking $m_{2,3}$ is close to the best marking ($m_{1,3}$) and is inconsistent: it has to be studied and tracked while estimating the system state. Indeed it allows to anticipate a possible conflict that may occur if the APPR button is not pressed in a near future. At time 230 most of the corrected particles are in p_2 and the APPR button has been pressed (according to the observation): a safe state is recovered.

Conclusion

The particle Petri net-based estimation principle that is presented in this paper paves the way to the detection of inconsistent behaviors in systems subjected to discrete actions – e.g. human actions in a human–robot team.

Ongoing work is focusing on the analysis of the correction graph, and more specifically on inconsistent states. What is considered is to study the dynamics of inconsistent states within the correction graph while monitoring the system in order to design an *automatic monitoring agent* for hybrid systems that would allow an early detection of conflicts and if necessary the possibility to change the autonomy/control level of the robot/human agents to face dangerous situations or communication loss.

Experiments are being prepared with the flight simulator at Supaero in order to assess conflict detection in procedures involving complex autopilot modes.

References

Arulampalam, S.; Maskell, S.; Gordon, N.; and Clapp, T. 2002. A Tutorial on Particle Filters for Online Nonlinear/Non-Gaussian Bayesian Tracking. *IEEE Transactions on Signal Processing* 50(2):174–188.

Barrouil, C. 1993. Planification et analyse d'échec. In Fargeon, C., and Quin, J.-P., eds., *Robotique mobile*. Teknea. chapter 10.1, 275–288.

Benazera, E., and Travé-Massuyès, L. 2003. The consistency approach to the on-line prediction of hybrid system configurations. In *ADHS'03*.

Benferhat, S.; Lagrue, S.; and Papini, O. 2005. Revision of partially ordered information: axiomatisation, semantics and iteration. In *IJCAI'05*.

Bradshaw, J.; Sierhuis, M.; Acquisti, A.; Feltovich, P.; Hoffman, R.; Jeffers, R.; Prescott, D.; Suri, N.; Uszok, A.; and van Hoof, R. 2003. Adjustable autonomy and human-agent teamwork in practice: an interim report on space applications. In Hexmoor, H.; Castelfranchi, C.; and Falcone, R., eds., *Agent Autonomy*. Kluwer. chapter 11, 191–220.

Brookshire, J.; Singh, S.; and Simmons, R. 2004. Preliminary results in sliding autonomy for coordinated teams. In *Interaction between humans and autonomous systems over extended operations*, AAAI Spring Symposium, 127–132.

Chachoua, M., and Pacholczyk, D. 2000. A symbolic approach to uncertainty management. *Applied Intelligence* 13(3):265–283.

Clough, B. 2002. Metrics, Schmetrics! How the heck do you determine a UAV's autonomy anyway? In *Performance Metrics for Intelligent Systems Workshop*.

David, R., and Alla, H. 2005. *Discrete, continuous, and hybrid Petri nets*. Springer.

Del Vecchio, D., and Murray, R. 2004. Discrete state estimators for a class of hybrid systems on a lattice. In *HSCC'04*.

Doucet, A.; de Freitas, N.; Murphy, K.; and Russell, S. 2000. Rao-Blackwellised particle filtering for dynamic Bayesian networks. In *UAI'00*.

Drury, J.; Scholtz, J.; and Yanco, H. 2003. Awareness in human-robot interactions. In *IEEE Conference on Systems, Man and Cybernetics*.

Endsley, M. 2000. Theoretical underpinnings of situation awareness: a critical review. In Endsley, M., and Garland, D., eds., *Situation awareness analysis and measurement*. Lawrence Erlbaum Associates.

Fong, T.; Thorpe, C.; and Baur, C. 2003. Robot, asker of questions. *Robotics and Autonomous Systems* 42(3-4):235–243.

Goodrich, M.; Olsen, D.; Crandall, J.; and Palmer, T. 2001. Experiments in adjustable autonomy. In *IJCAI'01 Workshop on Autonomy, Delegation and Control: interacting with autonomous agents*.

Hofbaur, M., and Williams, B. 2002. Mode estimation of probabilistic hybrid systems. In *HSCC'02*.

Huang, H.-M.; Messina, E.; Wade, R.; English, R.; Novak, B.; and Albus, J. 2004. Autonomy measures for robots. In *Proceedings of the IMECE: International Mechanical Engineering Congress*.

Koutsoukos, X.; Kurien, J.; and Zhao, F. 2003. Estimation of distributed hybrid systems using particle filtering methods. In *HSCC'03*.

Lehmann, E. 2003. Particle filter. Ph.D. Coursework, Australian National Unversity.

Lerner, U., and Parr, R. 2001. Inference in hybrid networks: theoretical limits and practical algorithms. In *UAI'01*.

Lesire, C., and Tessier, C. 2005. Particle Petri nets for aircraft procedure monitoring under uncertainty. In *ATPN'05*.

Martin, C.; Schreckenghost, D.; and Bonasso, R. 2004. Augmenting automated control software to interact with multiple humans. In *Interaction between Humans and Autonomous Systems over Extended Operation*, AAAI Spring Symposium.

Nielsen, T., and Jensen, F. 2005. Alert systems for production plants: a methodology based on conflict analysis. In *ECSQARU'05*.

Scholtz, J. 2003. Theory and evaluation of human robot interactions. In *HICSS'03, 36th Annual Hawaii International Conference on System Sciences*.

Tomlin, C.; Mitchell, I.; Bayen, A.; and Oishi, M. 2003. Computational techniques for the verification of hybrid systems. *IEEE* 91.

Veeraraghavan, H., and Papanikolopoulos, N. 2004. Combining multiple tracking modalities for vehicle tracking in traffic intersections. In *ICRA'04*.

Yanco, H., and Drury, J. 2002. A taxonomy for human-robot interaction. In *AAAI'02 Fall Symposium on Human-Robot Interaction*.